Engineered DNA plasmid reduces immunity to dystrophin while improving muscle force in a model of gene therapy of Duchenne dystrophy

Peggy P. Ho[a], Lauren J. Lahey[b,c], Foteini Mourkioti[d,1,2,3], Peggy E. Kraft[d], Antonio Filareto[d], Moritz Brandt[d], Klas E. G. Magnusson[d], Eric E. Finn[e,f,g], Jeffrey S. Chamberlain[e,f,g], William H. Robinson[b,c], Helen M. Blau[d], and Lawrence Steinman[a,4]

[a]Department of Neurology, Stanford University, Stanford, CA 94304; [b]Department of Medicine, Division of Immunology and Rheumatology, Stanford University, Stanford, CA 94304; [c]Department of Medicine, Division of Immunology and Rheumatology, Veteran Affairs Palo Alto Health Care System, Palo Alto, CA 94304; [d]Baxter Laboratory for Stem Cell Biology, Department of Microbiology and Immunology, Institute for Stem Cell Biology and Regenerative Medicine, Stanford University, Stanford, CA 94305; [e]Department of Neurology, Senator Paul D. Wellstone Muscular Dystrophy Cooperative Research Center, University of Washington, Seattle, WA 98195; [f]Department of Medicine, Senator Paul D. Wellstone Muscular Dystrophy Cooperative Research Center, University of Washington, Seattle, WA 98195; and [g]Department of Biochemistry, Senator Paul D. Wellstone Muscular Dystrophy Cooperative Research Center, University of Washington, Seattle, WA 98195

Contributed by Lawrence Steinman, July 22, 2018 (sent for review May 22, 2018; reviewed by Emanuela Gussoni and Reinhard Hohlfeld)

In gene therapy for Duchenne muscular dystrophy there are two potential immunological obstacles. An individual with Duchenne muscular dystrophy has a genetic mutation in dystrophin, and therefore the wild-type protein is "foreign," and thus potentially immunogenic. The adeno-associated virus serotype-6 (AAV6) vector for delivery of dystrophin is a viral-derived vector with its own inherent immunogenicity. We have developed a technology where an engineered plasmid DNA is delivered to reduce autoimmunity. We have taken this approach into humans, tolerizing to myelin proteins in multiple sclerosis and to proinsulin in type 1 diabetes. Here, we extend this technology to a model of gene therapy to reduce the immunogenicity of the AAV vector and of the wild-type protein product that is missing in the genetic disease. Following gene therapy with systemic administration of recombinant AAV6-microdystrophin to mdx/mTR^{G2} mice, we demonstrated the development of antibodies targeting dystrophin and AAV6 capsid in control mice. Treatment with the engineered DNA construct encoding microdystrophin markedly reduced antibody responses to dystrophin and to AAV6. Muscle force in the treated mice was also improved compared with control mice. These data highlight the potential benefits of administration of an engineered DNA plasmid encoding the delivered protein to overcome critical barriers in gene therapy to achieve optimal functional gene expression.

Duchenne muscular dystrophy | gene replacement therapy | DNA plasmid | microdystrophin | mdx/mTRG2 mice

Duchenne muscular dystrophy (DMD) is the most common and severe form of childhood muscular dystrophy that affects 1 of 5,000 live-born males (1, 2). In DMD, mutations within the Xp21 allele result in a marked reduction or complete absence of dystrophin that affects plasma membrane integrity in both skeletal and cardiac muscle fibers (3, 4). Confirmation of DMD includes serum creatine kinase (CK) levels at least 40 times normal levels, myopathy on electromyogram, and muscle histopathology with diverse fiber diameters, connective tissue proliferation, and signs of actively degenerating and regenerating myofibers (5). Onset of DMD begins during early childhood, with progressive muscle wasting leading to skeletal muscle loss. Patients become wheelchair-bound as teenagers and typically succumb from late-stage cardiac and respiratory failure in their third decade of life (6).

With no known cure, both gene therapy and stem cell transplantation have been attempted in DMD in the past 20 y (7). Because the dystrophin gene is one of the largest known human genes at 2.2 Mb and 79 exons, and occupies roughly 0.1% of the genome, the packaging capacities of viral vectors have limitations (8, 9). A minidystrophin gene, which ranges between 6 and 8 kb in size, was identified in a family with mild DMD and results in expression of one-half the size of full-length dystrophin, but is still too large to be packaged into a single recombinant adeno-associated viral (rAAV) vector (10, 11). Several versions of microdystrophin genes (<4.0 kb in size) delivered by rAAV vectors produce about one-third the size of full-length dystrophin and have been effective in reversing the dystrophic phenotype in animal models (12–14). The goal for rAAV vector gene replacement therapy in DMD is to achieve persistent transgene expression of dystrophin at therapeutic levels. However, the appearance of neutralizing antibodies and T cell host immune

Significance

Duchenne muscular dystrophy is a genetic disorder in which mutations in the dystrophin gene causes severe muscle wasting. A proposed treatment method involves systemic gene replacement therapy to introduce a functional dystrophin gene to the skeletal and cardiac muscles of the patient via rAAV6. A potentially serious problem may arise from immune recognition of dystrophin and the accompanying adeno-associated viral (AAV) vector. This unwanted immunity could interfere with successful long-term dystrophin expression by muscle cells. To suppress the unwanted immune response, a DNA vaccine was engineered to dampen immunity to both dystrophin and AAV6 capsid. Development of this engineered plasmid aims to improve gene replacement therapy and to overcome problems inherent with unwanted immunity to the encoded protein and to the delivery vector.

Author contributions: P.P.H., F.M., P.E.K., A.F., M.B., K.E.G.M., E.E.F., J.S.C., W.H.R., H.M.B., and L.S. designed research; P.P.H., L.J.L., F.M., P.E.K., A.F., M.B., K.E.G.M., E.E.F., J.S.C., and W.H.R. performed research; P.P.H., L.J.L., F.M., P.E.K., A.F., M.B., K.E.G.M., J.S.C., W.H.R., H.M.B., and L.S. analyzed data; and P.P.H., F.M., A.F., J.S.C., W.H.R., H.M.B., and L.S. wrote the paper.

Reviewers: E.G., Boston Children's Hospital; and R.H., Institute of Clinical Neuroimmunology.

Conflict of interest statement: Stanford University has filed a provisional patent application on behalf of P.P.H. and L.S. claiming some of the concepts contemplated in this publication. L.S. and Reinhard Hohlfeld are coauthors on a 2017 Commentary.

See Commentary on page 9652.

[1]Present address: Department of Orthopedic Surgery, University of Pennsylvania, Philadelphia, PA 19104.

[2]Present address: Department of Cell and Developmental Biology, University of Pennsylvania, Philadelphia, PA 19104.

[3]Present address: Penn Institute of Regenerative Medicine, University of Pennsylvania, Philadelphia, PA 19104.

[4]To whom correspondence should be addressed. Email: steinman@stanford.edu.

This article contains supporting information online at www.pnas.org/lookup/suppl/doi:10.1073/pnas.1808648115/-/DCSupplemental.

Published online September 4, 2018.

responses to AAV capsid and to dystrophin transgene products have been noted, in both animal and human clinical trials, reducing the expression of dystrophin in muscle (15–17).

The *mdx* mouse model has a spontaneous X-chromosome–linked point mutation in the dystrophin gene, leading to near-complete absence of dystrophin protein (18). This mouse has high serum levels of CK and pyruvate kinase, markers of myopathy (18, 19). However, there are only mild skeletal muscle defects in the *mdx* model, suggesting that the model may best reflect Becker muscular dystrophy (20). Moreover, there are frequent dystrophin^{+} myofibers, representing somatic reversion or suppression of the *mdx* (21). Because a major difference between mice and humans is the length of their telomeres, the protective ends of chromosomes, a "humanized" second-generation double-knockout mdx/mTR^{G2} mouse model was developed, in which the lack of telomerase activity (mTR^{KO}) was combined with the *mdx* mutation (22). In this mdx/mTR^{G2} model, the regenerative capacity of myogenic stem cells was greatly reduced, as they more rapidly reached proliferative exhaustion. Moreover, these double-mutant mice not only exhibited many of the severe skeletal muscle phenotypic characteristics of human DMD that progressively worsened with age, but they also had a reduced incidence of dystrophin reversion in the myofibers and manifested the severe dilated cardiomyopathy and significantly reduced lifespans seen in patients (23, 24).

Engineered DNA plasmids to induce antigen-specific inhibition of immune responses in human autoimmune diseases have been developed in preclinical animal model settings (25–28). With this technology, specific inhibition of antigen-specific antibody and T cell responses have also now been described in clinical trials in humans with relapsing-remitting multiple sclerosis (MS) and type 1 diabetes mellitus (T1DM) (27, 29–32). When applied to autoimmune diseases with known antigen targets, this method may allow targeted reduction of unwanted antibody and T cell responses to autoantigens. Instead of taking therapeutic approaches where wide swathes of the immune response are suppressed, the approach with engineered DNA plasmids is a directed, antigen-specific approach to controlling unwanted adaptive immunity.

Our goal here was to diminish unwanted immune responses to dystrophin and AAV serotype-6 (AAV6) capsid to enhance gene replacement therapy. We showed that the addition of weekly microdystrophin tolerizing DNA vaccine injections over a 32-wk period reduced antibody reactivity to both dystrophin and AAV6 capsid, and that this enhanced muscle function.

Results

Study Design and Development of the Engineered Microdystrophin DNA Plasmid. We studied a systemically delivered AAV6-microdystrophin gene replacement therapy, and attempted to reduce its immunogenicity with an intramuscularly delivered engineered microdystrophin DNA plasmid vaccine. For gene replacement, we utilized an AAV expression vector encoding a 3.6-kb human microdystrophin cDNA that lacks a large portion of the rod domain and C-terminal domain of the full-size 11.2-kb dystrophin coding region, and cotransfected it with the pDGM6 packaging plasmid into HEK293 cells to generate rAAV6-microdystrophin vectors (33, 34). Systemic administration of the rAAV6-microdystrophin vector genomes effectively restores functional dystrophin production by providing persistent and widespread transduction in the respiratory, cardiac, and skeletal muscles (33–35).

For tolerization, defined as reducing adaptive immunity to the delivered gene product and to its vector, a DNA plasmid encoding microdystrophin was injected intramuscularly into the quadriceps of mice 1 wk after mice had been treated first with the rAAV6-microdystrophin gene vector given intravenously. Injection of the engineered DNA plasmid encoding microdystrophin was injected intramuscularly into the quadriceps of mice, weekly thereafter for 32 wk.

The construction of the engineered DNA plasmid encoding human microdystrophin (pBHT1CI-H3μDYS) was created by excising the 3,630-bp hinge 3 microdystrophin (ΔH2-R23+H3/ΔCT) cDNA from an AAV vector backbone plasmid (34) and inserting the cDNA into the 3,052-bp pBHT1CI plasmid backbone driven by a CMV promoter (Fig. 1*A*). The backbone of pBHT1CI contains a chimeric intron sequence, and has been further modified to decrease the number of immunostimulatory unmethylated bacterial CpG motifs (26, 27). These CpG motifs, that are recognized by Toll-like receptor 9 (TLR9), are substituted with immunosuppressive GpG motifs, which compete with CpG motifs for binding to TLR9 (26, 36).

Dystrophin deficiency combined with telomere dysfunction in the double-knockout mdx/mTR^{G2} mouse model results in severe muscular dystrophy phenotypic characteristics similar to DMD patients. Clinical manifestations are far greater than those seen in the more commonly used *mdx* model (22–24). In this study, asymptomatic 6-wk-old male mdx/mTR^{G2} mice were administered an intravenous bolus of 3×10^{12} vector genomes of rAAV6-microdystrophin for systemic gene delivery of human microdystrophin (33–35). Next, 0.25% bupivicaine-HCL was administered to both quadriceps to prime the muscles 2 d before engineered DNA plasmid delivery. Mice were then randomly divided into three groups of five mice each and injected intramuscularly into both quadriceps with either vehicle (1× PBS), empty vector (pBHT1CI), or the engineered human microdystrophin DNA plasmid (pBHT1CI-H3μDYS) (Fig. 1*B*). In sum, after delivery of the gene therapy intravenously, beginning 1 wk thereafter, these mice were given 32 weekly intramuscular injections of vehicle, pBHT1CI, or pBTH1CI-H3μDYS before termination at 38 wk of age (Fig. 1*C*).

Functional Assays Reveal Increased Muscle Force Measurements. The rapid and progressive wasting of striated muscle is a hallmark of DMD (37). By providing a functional microdystrophin transgene in combination with an engineered microdystrophin DNA plasmid, we sought to determine whether this could effectively restore the generation of muscle force in vivo. Force measurements by electrical stimulation of the sciatic nerve within the lateral gastrocnemius muscle were performed in situ on the anesthetized mice. The investigator performing the force measurements was blind to the identity of the treatment groups. We noted significantly increased force generation between the treatment groups when measuring both the specific twitch force (Fig. 1*D*) and specific tetanus force (Fig. 1*E*). The group treated with the engineered DNA plasmid pBHT1CI-H3μDYS performed best, with statistically significant differences in both force measurements compared with the vehicle and pBHT1CI control groups ($P < 0.05$).

Cardiac involvement in DMD results from extensive fibrosis primarily affecting the left ventricle, beginning with sinus tachycardia and leading to progressive left ventricular dilation, systolic dysfunction, and ventricular arrhythmias (38–40). Intravenous injection of rAAV6-microdystrophin vector genomes can effectively transduce both skeletal and cardiac muscles in *mdx* mice for up to 2 y (33, 35). At the end of this study, 38-wk-old male mdx/mTR^{G2} mice were anesthetized and tested for cardiac function by electrocardiography. The investigator performing the cardiac measurements was masked to the identity of the treatment groups. We found that the heart rates were significantly lower in all three treatment groups (*SI Appendix*, Fig. S1*A*), and the stroke volumes were notably higher in the vehicle group and in the pBHT1CI-H3μDYS group (*SI Appendix*, Fig. S1*B*) compared with naïve age-matched mdx/mTR^{G2} mice. However, at 38 wk of age, there was no difference in cardiac output between any of the groups. Moreover, even though the pBHT1CI-H3μDYS–treated mice had statistically higher left ventricular end diastolic volume (*SI Appendix*, Fig. S1*D*) and left ventricular end diastolic diameter (*SI Appendix*, Fig. S1*G*), there were no significant indications of cardiomyopathy between any of the three treatment groups versus the naïve group. These are indicated by both the percent ejection fraction (*SI Appendix*, Fig. S1*F*) and percent fractional shortening (*SI Appendix*, Fig. S1*I*).

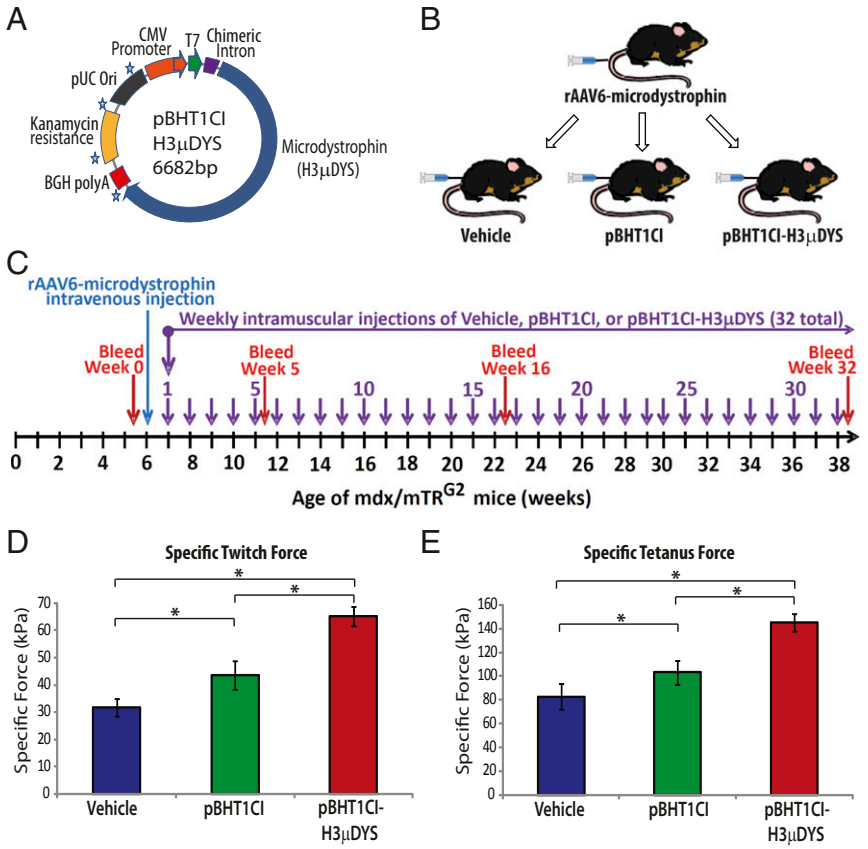

Fig. 1. Summary of study design and functional muscle force measurements. (*A*) Structural design of engineered DNA plasmid pBHT1CI-H3μDYS. pBHT1CI-H3μDYS is a 6.6-kb bacterial plasmid expression vector containing the coding sequences for microdystrophin gene. Important functional and control features of pBHT1CI-H3μDYS include the human CMV immediate-early gene promoter/enhancer, a chimeric intron sequence, a bovine growth hormone gene polyadenylation signal, a kanamycin resistance gene, and a pUC origin of replication for propagation of the vector in *E. coli*. The backbone of pBHT1CI-H3μDYS has been modified to decrease the number of immunostimulatory CpG sequences with substituted GpG immunosuppressive sequences (stars). (*B*) Schematic of the engineered DNA plasmid treatment groups following administration of rAAV6-microdystrophin. (*C*) Schematic of the study design. mdx/mTR^{G2} male mice were administered 3×10^{12} vector genomes of rAAV6-CMV-H3μDYS intravenously at 6 wk of age. Mice were then separated into three groups of five mice, and administered with either vehicle, empty control vector (pBHT1CI), or pBHT1CI-H3μDYS. Thirty-two weekly intramuscular injections were given to both hindlimbs. Blood samples were collected at weeks 0, 5, 16, and 32. (*D* and *E*) Muscle force was measured in the lateral gastrocnemius muscle in vivo in 38-wk-old anesthetized mice by electrical stimulation of the sciatic nerve and the generated force was recorded. Data show specific twitch force (*D*) and specific tetanus force (*E*) and are represented as average ± SEM ($n = 5$). *$P < 0.05$ by Student's *t* test.

Mice were quickly killed and blood, spleens, and gastrocnemius muscles were collected for further analysis. To investigate whether muscle functional improvement was accompanied by an increase in dystrophin$^+$ myofibers, cryosections of gastrocnemius muscle were stained using an antibody specific for human dystrophin. As expected, mice that received rAAV6-microdystrophin in combination with the engineered DNA plamsid pBHT1CI-H3μDYS showed a substantial presence of dystrophin$^+$ myofibers (*SI Appendix*, Fig. S2). Given that expression of therapeutic human microdystrophin protein is extremely robust in *mdx* mice for at least a year (33, 35), we did not expect to see significant differences in dystrophin staining between the treatment groups at 38 wk of age.

Serum CK levels, a measure of active muscle degeneration, are grossly elevated before onset of DMD clinical signs and decrease with the progression of the dystrophic process (41, 42). The mdx/mTR^{G2} model reflects this same trend when comparing between mice that were 8 wk vs. 60 wk of age (23). In this study, we did not see any statistically significant differences in CK levels in the pBHT1CI-H3μDYS–treated group in 36-wk-old mice after 30 wk of treatment (*SI Appendix*, Fig. S3).

T Cell Reactivity Detected to Two Distinct Epitopes Outside of the Microdystrophin Transgene. We sought to reduce immunogenicity to AAV and to immunogenic domains of dystrophin to overcome the potential deleterious immune responses to these potential antigens, responses that diminish the benefits expected from gene therapy. Because AAV-specific T cells have also been reported to produce IFN-γ, IL-2, and TNF-α in patients (43), we next measured plasma cytokine levels to determine if the mdx/mTR^{G2} mice may have developed a peripheral inflammatory cytokine signature following systemic delivery of rAAV6-microdystrophin vectors. The investigator performing this assay was blind to the identity of the treatment groups. Mice were sampled early (week 5) (Fig. 2*A*) and late (week 32) (Fig. 2*B*) in our study. Although there was a trend in decreased levels of IFN-γ, TNF-α, IL-6, and IL-17A within the pBHT1CI-H3μDYS–treated group compared with the vehicle group at the end of the study, overall these results were not statistically significant.

Spleens harvested from the mice were pooled into their respective treatment groups. A T cell proliferation assay was performed with overlapping 20-mer human dystrophin peptides, AAV6 capsid peptides, or control peptides, grouped in five peptides for a total of 62 groups for screening (*SI Appendix*, Table S1). We did not observe any robust T cell reactivity to any particular group of pooled peptides (Fig. 3*A*). However, we noted that peptide groups 23 and 33 that spanned human dystrophin amino acid sequences 1,651–1,730 and 2,401–2,480 (Fig. 3*B*) appeared to have a modest T cell response. This was also observed at an earlier timepoint, sampled after intravenous injections of rAAV6-microdystrophin vector genomes followed by only three weekly intramuscular injections of pBHT1CI-H3μDYS (*SI Appendix*, Fig. S4). Here, naïve mdx/mTR^{G2} mice also had similar modest T cell responses to the peptide groups 23 and 33 (*SI Appendix*, Fig. S4). Interestingly, these amino acid sequences are not part of the human microdystrophin sequence. The human microdystrophin cDNA includes amino acid sequences 1–677 and 2,942–3,408 of the total 3,685 amino acid sequence of human dystrophin. Overall homology between mouse and human dystrophin sequences is 91.6% shared amino acid identity (44). Peptide groups 23 and 33 share 89% and 84% homology, respectively, to the mouse peptide counterparts. Because the possibility of revertant myofibers still exists in the mdx/mTR^{G2} mice, these two groups of peptides may encompass the immune epitopes for an autoreactive T cell response against endogenous dystrophin. Cytokine analysis of the T cell supernatants by sandwich ELISA resulted in no statistically significant production of IFN-γ, TNF-α, IL-6, or IL-17 to any of the 62 peptide groups.

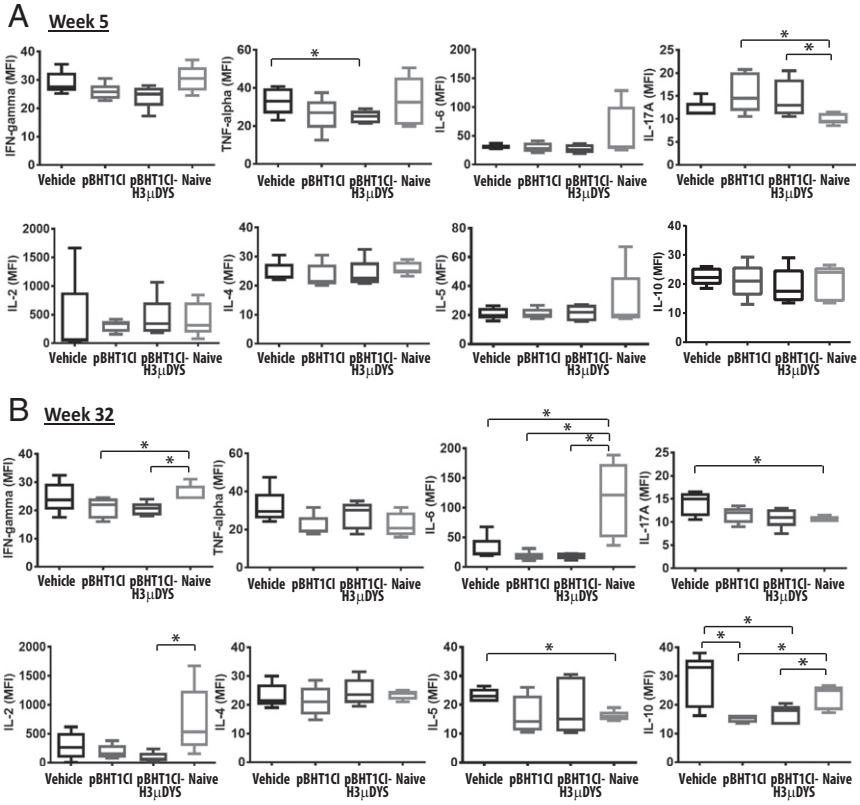

Fig. 2. Assessment of the peripheral inflammatory cytokine signature. Cytokine analysis by Luminex on plasma samples taken on (*A*) week 5 and (*B*) week 32 of the study. Values are shown as median fluorescence intensity (MFI). $*P < 0.05$ by Student's *t* test.

Engineered Microdystrophin DNA Plasmid Treatment Decreases Antibody Reactivity to Dystrophin and AAV6 Capsid. Following systemic gene replacement with rAAV6-microdystrophin vector genomes, serum samples were collected at 5, 16, and 32 wk during the weekly engineered DNA plasmid treatments (Fig. 1*C*). These samples were analyzed by microarray analysis for antibody production against dystrophin and AAV6 capsid protein, with matched week 0 (baseline) sera analyzed in parallel to establish the fold change in reactivity relative to baseline. The 1,404-feature proteomic arrays for dystrophin and AAV6 capsid contain

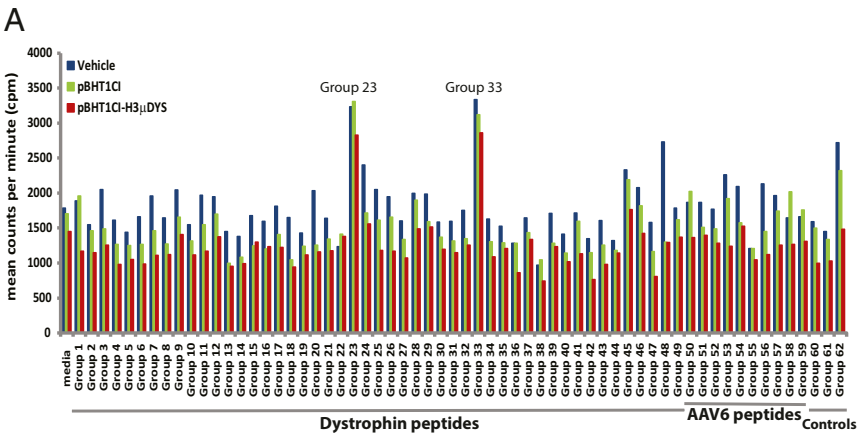

B

Group Name	Peptide Name	peptide sequence
Group 23	hu-Dyst 1651-1670	DKLSLLNSNWIAVTSRAEEW
	hu-Dyst 1666-1685	RAEEWLNLLLEYQKHMETFD
	hu-Dyst 1681-1700	METFDQNVDHITKWIIQADT
	hu-Dyst 1696-1715	IQADTLLDESEKKKPQQKED
	hu-Dyst 1711-1730	QQKEDVLKRLKAELNDIRPK
Group 33	hu-Dyst 2401-2420	RKLEDLSSEWKAVNRLLQEL
	hu-Dyst 2416-2435	LLQELRAKQPDLAPGLTTIG
	hu-Dyst 2431-2450	LTTIGASPTQTVTLVTQPVV
	hu-Dyst 2446-2465	TQPVVTKETAISKLEMPSSL
	hu-Dyst 2461-2480	MPSSLMLEVPALADFNRAWT

Fig. 3. T cell proliferation assay against human dystrophin and AAV6 capsid. Splenocytes collected at the end of the study were harvested, pooled, and stimulated with 20-mer overlapping peptides in groups of five that spanned the entire sequences for human dystrophin, AAV6 capsid, or control peptides for a total of 72 h. (*A*) ^{3}H-Thymidine incorporation was measured and mean counts per minute (cpm) of triplicate wells are shown. (*B*) Peptide sequences from the two groups of pooled human dystrophin peptides that showed modest T cell reactivity.

306 distinct antigens consisting of overlapping 20-mer peptide sequences representing human dystrophin, AAV6 capsid, and control peptides and proteins (*SI Appendix*, Table S1). The investigator performing the assay was blind to the identity of the treatment.

Arrays incubated with the collected serum revealed that mdx/mTR^{G2} mice developed an increasingly expanded antibody repertoire against epitopes derived from human dystrophin over time. The significance analysis of microarrays (SAM) algorithm was applied to identify antigen features with statistically significant differences in array reactivity between the treated groups (45). A hierarchical cluster algorithm, using a pairwise similarity function, was deployed to order SAM-selected antigen features based on degree of similarity in their antibody reactivity profiles (46). We set the q value (false-discovery rate) to reflect a direct comparison between the vehicle and pBHT1CI-H3μDYS groups. The data are presented as a heatmap.

At 5 wk, we found a limited antibody reactivity by SAM analysis against seven human dystrophin peptides that were generated by the vehicle-treated mice. These same antibody responses were notably lower in the pBHT1CI-H3μDYS–treated mice (Fig. 4*A*) (q value = 34.9%). After 16 wk of tolerizing DNA vaccine treatment, SAM analysis revealed antibodies against 42 human dystrophin peptides in the vehicle-treated mice that were again decreased in the pBHT1CI- H3μDYS–treated mice (Fig. 4*B*) (q value = 3.4%). Finally at the end of the study, after 32 wk of tolerizing DNA vaccine treatment, SAM analysis identified strong antibody reactivity against 66 human dystrophin peptides in the vehicle-treated mice that were predominantly diminished in the pBHT1CI- H3μDYS–treated mice (Fig. 4*C*) (q value = 4.5%). During all three time points assayed, the pBHT1CI empty vector control group had antibody reactivities that always ranged between the vehicle-treated group and the pBHT1CI-H3μDYS–treated group. Because the vector backbone contains immunosuppressive GpG sequences, treatment with just the pBHT1CI empty vector alone may be providing an additional nonspecific antiinflammatory effect (26, 36).

Peptide sequences identified by SAM analysis were further grouped into those that encompassed human microdystrophin versus those that were from the remaining regions of full-length human dystrophin (Fig. 4). At all three timepoints, the antibody repertoire reacted to epitopes that are both within and outside of microdystrophin. Whether this immune response was due to revertant myofibers, or enhanced due to the introduction of the microdystrophin transgene, cannot be determined at this time. Nevertheless, the data indicate that the engineered microdystrophin DNA plasmid suppressed the antibody responses to regions of both microdystrophin and full-length dystrophin. We also summarize the evolution of the initial seven peptides targeted by antibodies at week 5 and follow them through weeks 16 and 32 to highlight the efficacy of the engineered DNA plasmid in dampening the B cell response (*SI Appendix*, Fig. S5).

Finding antibody reactivity to the AAV6 capsid protein was also a distinct possibility given that a rAAV6 viral vector was used for systemic microdystrophin gene delivery (33). Mice surveyed at week 5 (Fig. 5*A*), week 16 (Fig. 5*B*), and week 32 (Fig. 5*C*) also developed an increasingly expanded antibody repertoire against peptide sequences specific for AAV6 capsid that were detectable in vehicle-treated mice and diminished in pBHT1CI-H3μDYS–treated mice. Once again, the pBHT1CI empty vector control group had moderate antibody responses against AAV6 capsid peptide sequences. Here we are able to show that mice treated with systemic rAAV6-microdystrophin gene replacement develop antibodies against AAV6 capsid over time. Moreover, we also show that engineered DNA plasmid treatment reduced this antibody response to AAV6 capsid determinants.

Discussion

In DMD patients, exons 3–5 and 45–55 of the dystrophin gene are hotspot regions for mutations that can effectively disrupt the reading frame of dystrophin mRNA (4, 47). This results in a prematurely truncated and unstable dystrophin protein that emanates in the dystrophic phenotype. Current gene therapy methods to restore dystrophin gene expression include gene repair, exon skipping, and gene replacement. Clustered regularly interspaced short palindromic repeat (CRISPR)/Cas9 technology (48) generates targeted deletions within the mutated exon to restore the dystrophin reading frame. Thus, CRISPR/Cas9 genome editing permanently corrects the defect in the dystrophin gene rather than just transiently adding a functional dystrophin gene. This technology is still in preclinical developmental stages for the treatment of DMD amid concerns with immune responses to both the bacterial-derived Cas9 protein and to the AAV expression vector, and concerns with a high frequency of off-target cutting (48–53).

With exon skipping, antisense oligonucleotides serve as structural analogs of DNA that allow faulty parts of the dystrophin gene to be skipped when it is transcribed to RNA for protein production (54). The downside with exon skipping is that it does not permanently repair the mutated dystrophin gene and requires repeated delivery of mutation-specific antisense oligonucleotides or the transfer of transfected muscle satellite stem cells (47, 54, 55).

Myoblast cell transplantation as a method of gene transfer was initially promising in the *mdx* mouse model of DMD (56). Intramuscular injections of normal myoblasts into *mdx* mice formed mosaic muscle fibers that expressed the normal dystrophin gene from the implanted myoblasts (56–58). Several subsequent human clinical trials with myoblast-mediated gene transfer as therapy for DMD patients produced detectable dystrophin transcripts from donor myoblasts derived from a male relative (59–63). However, the efficiency of donor myoblast implantation and myofiber transduction in human DMD patients remained low (56).

The long-term goal in DMD is to replace the defective or missing dystrophin protein. One of the problems with effectively replacing dystrophin in attempts at gene therapy is an unwanted immune response to dystrophin or its orthologs that are recognized as neoantigens (35, 64, 65). Braun et al. (15) reported on the immune rejection of human dystrophin following intramuscular administration of a full-length human dystrophin *Escherichia coli* plasmid in *mdx* mice. Both B cell and weak T cell responses against the human dystrophin protein found 21 d following plasmid injection coincided with transient myositis. Maximal dystrophin expression was detected at 7 d, but expression waned by day 28, even after boosting on day 21 (15).

Mendell et al. (17) found modest dystrophin-specific T cell immunity in patients with DMD both before and after gene therapy in a human clinical trial. A small clinical trial of six DMD patients received a single dose of either 2×10^{10} or 1×10^{11} of a functional rAAV2-minidystrophin transgene delivered intramuscularly to one bicep. Only two of the six patients had detectable dystrophin in the injected myofibers after 6 wk, indicating a failure to establish long-term transgene expression. Surprisingly, peripheral T cells specific for dystrophin were discovered in two other patients before vector treatment, which was presumed due to the expression of dystrophin in revertant muscle fibers (17, 66).

Another obstacle that occurs when a viral vector is systemically administered for gene replacement therapy is the immunogenicity of the AAV capsid that can also be detected in patients (16). Indeed, Manno et al. (67) reported successful transduction of liver by rAAV2-factor IX in hemophilia patients that then gradually declined over a period of about 8 wk due to T cell-mediated immunity specifically targeting AAV capsid antigens. Studies in preclinical animal models showed long-lasting therapeutic expression of factor IX (67–70). The anti-AAV immune response following systemic viral vector delivery is likely triggered from memory responses to prior wild-type AAV exposure. Natural infection with wild-type AAV occurs widely among humans and not typically found in research animals (43).

Thus, a technology that could induce immunological tolerance to specific antigens, whether dystrophin or AAV capsid proteins,

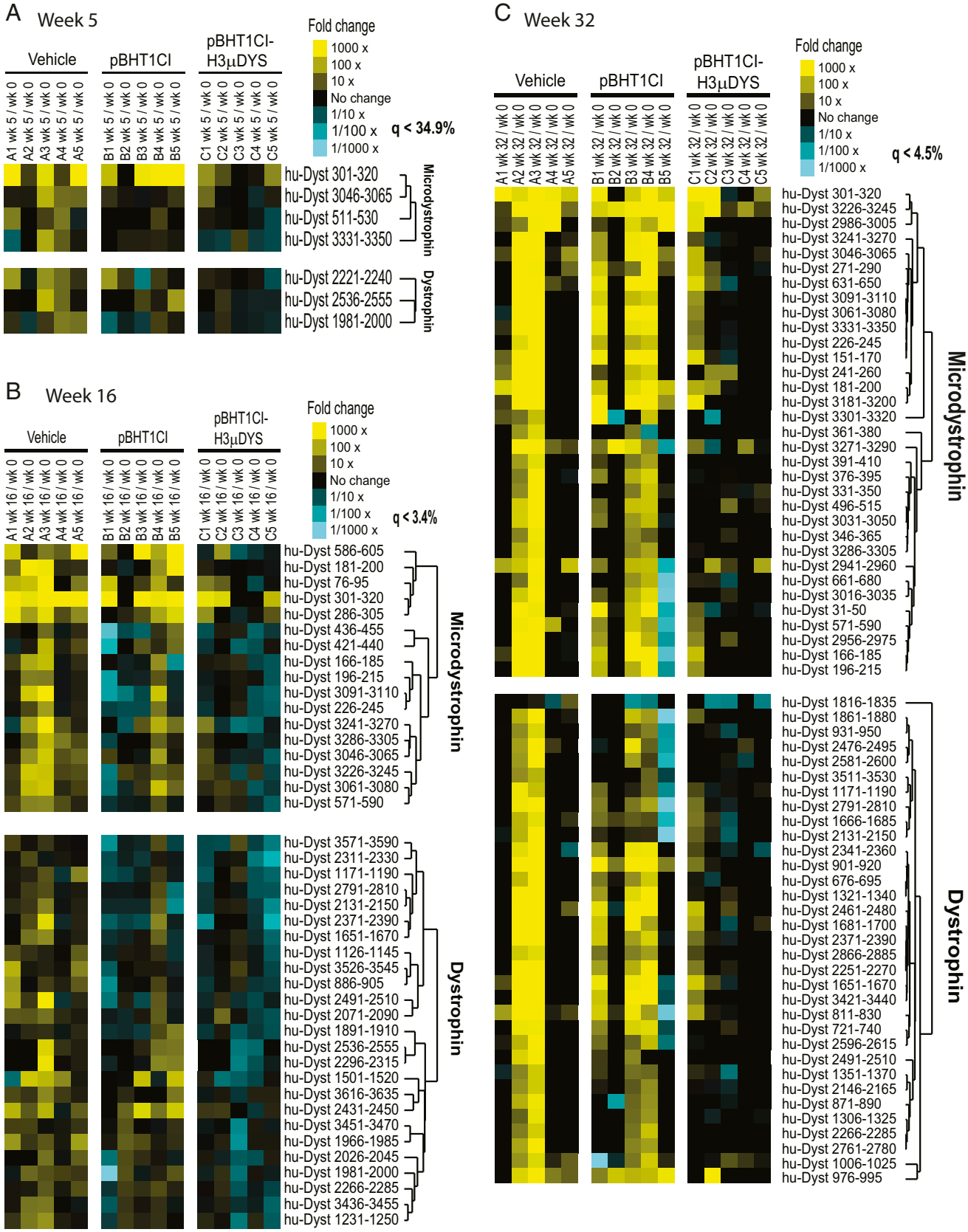

Fig. 4. Hierarchical clustering of antigen features in human dystrophin proteome array reactivity between sera derived from vehicle-, pBHT1CI-, or pBHT1CI-H3μDYS–treated mice. Heatmaps representing antibody reactivity to human dystrophin peptides are shown as fold-change from baseline (week 0). (*A*) Week 5: vehicle vs. pBHT1CI-H3μDYS (q value = 34.9%). (*B*) Week 16: vehicle vs. pBHT1CI-H3μDYS (q value = 3.4%). (*C*) Week 32: vehicle vs. pBHT1CI-H3μDYS (q value = 4.5%).

will likely be necessary for effective gene replacement therapy. Over the past decade, our group has shown proof-of-concept for this approach in animal models of MS and T1DM (25–28), and has taken the program into human trials in relapsing-remitting MS, in 280 patients (30, 32), and in T1DM, in 80 patients (31).

Here we explored how we might tolerize to immunogenic domains of dystrophin and to AAV, to overcome two of the existing obstacles hindering the long-term success of gene therapies for DMD. We refer to tolerization here as reduction of the adaptive immune response to the wild-type protein, or to the "miniprotein" encoded in the viral vector. Tolerization also encompasses reduction of the response to the viral capsid proteins.

In this study, systemic gene replacement with rAAV6-microdystrophin vectors into 6-wk-old mdx/mTR^{G2} mice restored expression of dystrophin for up to 38 wk of age. The addition of weekly intramuscular injections of an engineered microdystrophin DNA plasmid, pBHT1CI-H3μDYS, significantly increased the generation of muscle force compared with control-treated mice. This observation suggested the possibility that antigen-specific therapy may be aiding in the effective expression of the microdystrophin transgene by suppressing aberrant immune response against the rAAV6-microdystrophin vector.

Early studies by our group reported that mdx/mTR^{G2} mice have markedly decreased muscle force as early as 8 wk of age, developed severe functional cardiac deficits as early as 32 wk of age, and had elevated serum CK levels at 8 wk of age that declined by 60 wk of age (23, 24). mdx/mTR^{G2} mice also have significantly reduced lifespans, with death occurring as early as 48 wk of age with a t_{50} of 80 wk of age (23, 24).

Although several of the other functional assays in the present study showed no significant differences between the treatment groups, future studies where the treated mdx/mTR^{G2} mice are followed beyond 60 wk of age, at which point many of the severe dystrophic phenotypes are more pronounced, would potentially aid in determining the additional benefits of this combination treatment.

It is noteworthy that such a robust expression of dystrophin in AAV6-microdystrophin–treated animals did not result in decreased CK values. Serum CK levels decrease as *mdx* mice age, and similar decreases in CK are seen in older humans with DMD. In addition, CK levels can be elevated in mice that are handled a lot, and in mice who move around significantly. While AAV vectors are quite useful for systemic delivery, there are significant differences in transduction between individual muscles. The best improvement of CK levels was observed in AAV-treated older *mdx* mice. Even then, only a 90% reduction in serum CK levels was attained in mice that were 2-y-old (71). In that study it should be noted that 10^{13} vector genomes were administered, a higher dose than used here.

Many dystrophin^{+} fibers still have centrally located nuclei, suggesting that despite restoration of dystrophin expression in these fibers, histological correction did not occur and myonuclei were not relocated to the periphery. Reversal of central nucleation is a very slow process. Until recently centrally located nuclei was considered an irreversible phenotype. However, in one of the few studies to directly test this issue we found that central nucleation could be slowly reduced in AAV-microdystrophin–injected tibialis anterior muscles of *mdx* mice (14). Interestingly, in that study the reversal of central nucleation occurred over many months, but by 6-mo postinjection nearly 15% of myofibers still displayed central nucleation. Thus, our data suggest that this architectural abnormality of dystrophic muscle can be ameliorated, but it is a slow process.

Adaptive immune responses to dystrophin and to the capsid proteins of the vector encoding dystrophin have been seen in studies of gene therapy of DMD in preclinical models. Weak T cell responses to human dystrophin were detectable, and IFN-γ production in *mdx* mice was observed at 42 d after intramuscular injection of a plasmid containing full-length human dystrophin (15). AAV2 and AAV8 capsid-specific CD8^{+} IFN-γ–producing T cells were identified by flow cytometry in mice 9 d after injection of AAV2 VP1 capsid or AAV8 VP1 capsid, respectively (72).

Here we did not detect any robust T cell responses specifically toward the microdystrophin transgene or to AAV6 capsid using ^{3}H-thymidine uptake to measure the T cell responses to overlapping peptides. However, we did find weak T cell reactivity against two regions of dystrophin, p1651–1730 and p2401–2480, which were outside of the microdystrophin transgene. We hypothesize that this dystrophin-specific T cell reactivity may already have been generated against endogenous dystrophin in revertant myofibers or other nonmuscle dystrophin isoforms that could still be expressed in the mdx/mTR^{G2} mice, similar to what Mendell et al. (17) found in two patients. Cytokine analysis of the T cell supernatants by sandwich ELISA did not detect any notable production of IFN-γ, TNF-α, IL-6, or IL-17 to AAV6 capsid or dystrophin, including the two T cell-reactive regions of dystrophin, p1651–1730 and p2401–2480. We found that several inflammatory cytokines, including IFN-γ and IL-6, were modestly reduced but not with statistical significance following combination therapy.

Humoral immune responses to AAV capsid proteins have been previously reported histologically in both wild-type and *mdx* muscle following intramuscular injection of the AAV vector (73, 74). Dystrophin antibodies have also been detected by Western blot analysis following intramuscular injection of full-length human dystrophin plasmid DNA into *mdx* mice (75). Here, we used our proteomic array technology to profile the evolution of peripheral antibody responses to dystrophin and AAV6 capsid following human microdystrophin gene replacement in mdx/mTR^{G2} mice. Over the course of the 32-wk study, we measured the expansion of adaptive antibody responses to both dystrophin and to AVV6 capsid in mdx/mTR^{G2} mice that received AVV6-microdystrophin gene replacement. Mice that were also treated with the engineered microdystrophin DNA plasmid had notably reduced antibody responses both to microdystrophin and to other regions of full-length dystrophin, as well as to epitopes of AAV6 capsid.

These data were surprising to us, as we had initially planned on including a second engineered DNA plasmid containing the AAV6 capsid cDNA as part of the combination therapy, to directly suppress the immune response to AAV6. We can rationalize this unexpected and encouraging observation, in part, as due to the vector effect, given that our pBHT1CI empty vector control-treated group also showed improvement over the vehicle control group in three measurements, including: (*i*) increased generation of muscle force, (*ii*) increased expression of dystrophin immunohistochemically, and (*iii*) in reduction of antibodies against dystrophin and AAV6 capsid. Unmethylated bacterial CpG motifs, which trigger an inflammatory innate immune response through the TLR9 signaling pathway, are found within the rAAV6-microdystrophin vector due to the necessity of having to initially grow the AAV-microdystrophin expression vector in bacterial cultures (76). Our modified pBHT1CI plasmid backbone contains several engineered antiinflammatory GpG motifs that, by themselves, can nonspecifically suppress the CpG mediated proinflammatory immune response (36). Another possibility is that tolerizing DNA vaccines may activate CD4^{+} CD25^{+} T regulatory cells and induce a shift from proinflammatory Th1 cells to antiinflammatory Th2 cells (77). These other immunomodulatory mechanisms could also mediate tolerance to the AAV components in the rAAV6-microdystrophin gene therapy vector.

Timing of the tolerization protocol may be critical, and earlier intervention may be warranted. Typically, *mdx* mice go through a period of strong degeneration/regeneration at 2–3 wk of age, with increased inflammation reported during this time. Such muscle remodeling/increased inflammation might trigger some of the observed reactivity to dystrophin in regions that would only be expressed by revertant fibers. Beginning tolerization at even 1 wk of age may obviate this inflammatory response.

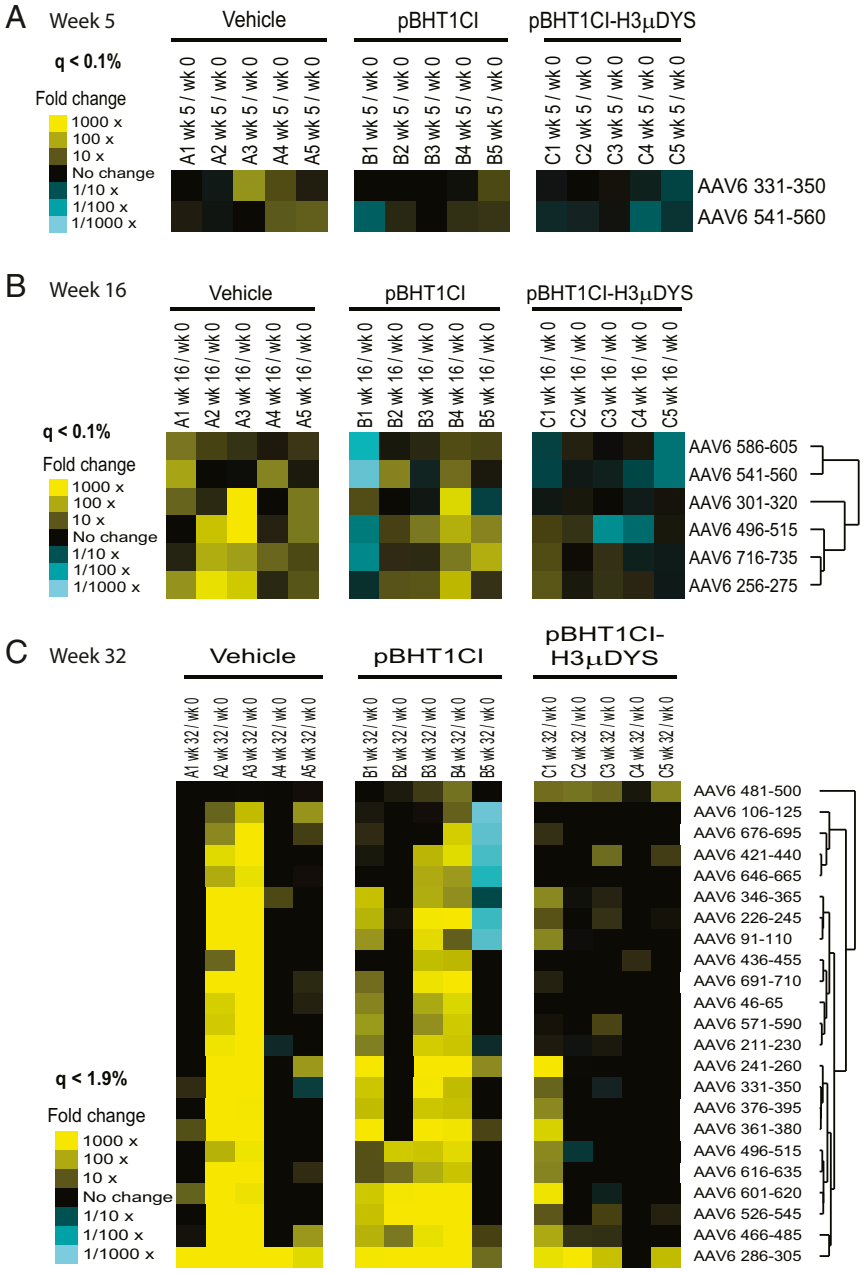

Fig. 5. Hierarchical clustering of antigen features in AAV6 capsid proteome array reactivity between sera derived from vehicle-, pBHT1CI-, or pBHT1CI-H3μDYS–treated mice. Heatmaps representing antibody reactivity to AAV6 capsid peptides are shown as fold-change from baseline (week 0). (*A*) Week 5: vehicle vs. pBHT1CI-H3μDYS (q value < 0.1%). (*B*) Week 16: vehicle vs. pBHT1CI-H3μDYS (q value < 0.1%). (*C*) Week 32: vehicle vs. pBHT1CI-H3μDYS (q value < 1.9%).

In conclusion, to retain persistent transgene expression at therapeutic levels for DMD, AAV-based gene therapy may need to be coupled with immunosuppression. Indeed, several forms of immunosuppression have already been demonstrated in DMD animal models to successfully dampen the cellular responses against AAV. These current treatments, including anti-CD4 antibody, antithymocyte globulin, cyclosporine, prednisone, tacrolimus, mycophenolate mofetil, and plasmapheresis all broadly suppress the immune system, which would not be ideal for young DMD patients (16, 69, 70, 78). We offer, instead, a well-tolerated antigen-specific therapeutic technology that can now be included with gene replacement therapy for DMD and other inherited genetic mutations, such as retinal dystrophy or hemophilia. Thus, overcoming a known deleterious issue with gene replacement therapy may be resolved with DNA plasmids engineered to reduce immunity to the viral vector and to the protein delivered by the transgene.

Materials and Methods

Generation of Constructs.

rAAV6-microdystrophin. The rAAV6-CK8-coh-H3μDYS (rAAV6-microdystrophin) vector comprising serotype 6 capsids was generated by cotransfecting the "hinge 3" codon-optimized human microdystrophin pAAV CK8e-coh-H3μDYS expression vector (34) together with the pDGM6 packaging plasmid into HEK293 cells. The rAAV6-microdystrophin vector genomes were harvested, purified, and quantitated as previously described (33, 35).

Engineered DNA plasmid. The "hinge 3" codon-optimized human microdystrophin pAAV CK8e-coh-H3μDYS expression vector (8162 bp) was digested with XhoI and HpaI to isolate the H3μDYS microdystrophin gene with the "Ck8e" small enhancer plus promoter sequence (3,630 bp) (34, 35). This "Ck8e" human microdystrophin cDNA includes amino acid sequences 1–677 and 2,942–3,408 of the total 3,685-amino acid sequence of human dystrophin (34). The engineered DNA vector (pBHT1CI) was digested with HindIII and XhoI (3,052 bp). The function and control features of BHT1CI include the human cytomegalovirus immediate-early gene promoter/enhancer, a chimeric intron sequence, a bovine growth hormone gene polyadenylation signal, a kanamycin resistance gene, and a pUC origin of

replication for propagation of the vector in *E. coli* (31). Additionally, the backbone of pBHT1CI has been modified to decrease the number of immunostimulatory CpG sequences and substituted with immunosuppressive sequences (26, 36). The complete engineered human microdystrophin DNA plasmid (pBHT1CI-H3μDYS) is 6,682 bp. Purification of engineered DNA plasmids were described previously (28).

Animal Care. Protocols were approved by the University Administrative Panel (Institutional Animal Care and Use Committee A3213-01, 27080, 11090). Male mdx/mTR^{G2} and C57BL/6 mice were bred and housed at Stanford University.

Manipulation of Experimental Mice. Asymptomatic 6-wk-old male mdx/mTR^{G2} mice (23) were administered 0.2 mL of 3×10^{12} rAAV6-microdystrophin vector genomes in HBSS into the tail vein (33). Five days later, both quadriceps were injected intramuscularly with a total of 0.1 mL of 0.25% bupivicaine-HCL (Sigma-Aldrich) in PBS. Two days later, the mice were injected intramuscularly into both quadriceps with 0.1 mg pBHT1CI or pBHT1CI-H3μDYS in a volume of 0.1 mL PBS. Mice were given 32 weekly injections of 1× PBS (vehicle), pBHT1CI, or pBTH1CI-H3μDYS (five mice per group). Mice were bled retro-orbitally before systemic delivery of the rAAV6-microdystrophin vector genomes (baseline), then 5, 16, and 32 wk after. Whole blood was submitted to the Animal Diagnostic Laboratory at the Stanford Medicine Veterinary Service Center for measurement of serum CK levels by immunoassay at treatment week 30.

Echocardiographic Analysis of Cardiac Function. Anesthesia of mice was induced in a chamber (2–4% isoflurane mixed with 0.2 L/min 100% O_2) and maintained with a face mask (1–2% isoflurane with 0.2 L/min 100% O_2). Animals were depilated and kept on a heated table mounted on a rail system (Visual Sonics). Ultrasound was performed with a Vevo 2100 System and a 22- to 55-MHz mouse transducer (VisualSonics). Heart rate and body temperature were monitored and maintained at physiological levels. B-mode and M-mode images were recorded at the papillary muscle level. Left ventricular wall thickness, intraventricular septum thickness, left ventricular end-diastolic and end-systolic volumes, left ventricular volumes, fractional shortening, ejection fraction, and cardiac output were calculated.

Force Measurements. The 38-wk-old male mdx/mTR^{G2} mice were anesthetized and force measurements by electrical stimulation of the sciatic nerve within the lateral gastrocnemius muscle were performed in situ, and expressed relative to cross-sectional area, as previously described (23), in accordance with approved Stanford University guidelines.

Immunofluorescence of Tissue Sections. Harvested gastrocnemius muscles were embedded in Tissue-Tek OCT compound and flash-frozen in isopentane cooled in liquid nitrogen. Staining is described elsewhere (79). Primary antibodies used were anti-human DMD polyclonal antibody produced in rabbit (HPA0002725, 1:500; Sigma Aldrich) and rabbit anti-Laminin antibody (1:400; Sigma). Secondary antibodies used were goat anti-rabbit antibody Alexa 555 and goat anti-rabbit antibody Alexa-488 (1:1,000; Molecular Probes). DAPI (1:5,000; Sigma) was used to counter stain the nuclei. Representative images of transverse sections of gastrocnemius muscles from the indicated treatment groups at 38 wk of age were immunostained for laminin (green), human dystrophin (red), and nuclei (blue).

Luminex–eBioscience/Affymetrix Magnetic Bead Kits. This assay was performed by the Human Immune Monitoring Center at Stanford University. Mouse 38-plex kits were purchased from eBiosciences/Affymetrix and used according to the manufacturer's recommendations, with modifications as described online at iti.stanford.edu/himc/protocols.html.

T Cell Proliferation Assay. Splenocytes were harvested, pooled, and stimulated in triplicate wells with 20-mer overlapping peptides in groups of five that spanned the entire sequences for human dystrophin, AAV6 capsid or control peptides (PEPscreen; Sigma-Aldrich) for a total of 72 h. For the final 18–24 h of culture, 1 μCi of ^{3}H-thymidine was added to each well, and incorporation of radioactivity was measured by using a Betaplate scintillation counter. Cytokine assays were performed on culture supernatants after 72 h of culture by using the IL-10, IFN-γ, and TNF BD OptEIA Mouse ELISA kits (BD Biosciences) or Mouse IL-17 DuoSet ELISA Development kit (R&D Systems).

Dystrophin Microarrays. Dystrophin proteome arrays were produced using a robotic arrayer (ArrayIt LM210) to attach peptides and proteins to SuperEpoxy 2-coated slides (ArrayIt Corporation) in an ordered array. On each array were printed four replicate features of each peptide (PEPscreen; Sigma-Aldrich) or protein at 0.2 mg/mL in PBS with up to 30% DMSO. This array contained a total of 1,404 features that included 1,208 antigenic features and 196 control features. Arrays were circumscribed with a hydrophobic marker, blocked overnight at 4 °C in PBS containing 3% FBS and 0.5% Tween-20, incubated with 1:150 (weeks 5 and 16) or 1:300 (week 32) dilution of mouse serum in blocking buffer for 1 h at 4 °C, and washed twice for 20 min rotating in blocking buffer. Week 32 plasma (and matched week 0 plasma) were evaluated at a more dilute concentration in the final experiment due to the increased signal at this timepoint. Arrays were incubated with 0.4 μg/mL cyanin 3 dye (Cy3)-conjugated goat anti-mouse IgM/IgG (weeks 5 and 16) or 0.4 μg/mL Cy3-conjugated goat anti-mouse IgG (week 32) (Jackson Immunoresearch) for 45 min at 4 °C and then washed twice for 30 min in blocking buffer, twice for 30 min in PBS, and twice for 15 s in water. Arrays were spun dry and scanned with a Molecular Devices 4400A scanner using GenePix 7 software to determine the net median pixel intensities for individual features. Normalized median net digital fluorescence units (DFUs) represent median values from four identical antigen features on each array. The median fluorescence intensity of each feature above blank levels was calculated for experimental arrays, with any DFU value <10 set to 10. To represent increases or decreases in reactivity at a given treatment timepoint relative to naïve, the $\log_2$ fold-change in DFU was calculated for each mouse. SAM 4.0 was applied to identify antigens with statistically significant difference in array reactivity between vehicle-treated or tolerizing DNA vaccine-treated groups, with a fold-change threshold of 5× employed. SAM ranks each antigen on the basis of a score obtained by dividing the differences between the mean reactivities for each group by a function of their SDs, and then estimates a false-discovery rate for each antigen by permuting the repeated measurements between groups (45). SAM results were arranged into relationships using Cluster 3.0, and results were displayed using TreeView 1.1.5r2. Detailed protocols are published and are available online at https://web.stanford.edu/group/antigenarrays/.

ACKNOWLEDGMENTS. This work was supported by NIH Grant HL122332 (to J.S.C.) and Muscular Dystrophy Association Grant MD1218077 (to L.S.).

1. Mendell JR, et al. (2012) Evidence-based path to newborn screening for Duchenne muscular dystrophy. *Ann Neurol* 71:304–313.
2. Moser H (1984) Duchenne muscular dystrophy: Pathogenetic aspects and genetic prevention. *Hum Genet* 66:17–40.
3. Koenig M, et al. (1987) Complete cloning of the Duchenne muscular dystrophy (DMD) cDNA and preliminary genomic organization of the DMD gene in normal and affected individuals. *Cell* 50:509–517.
4. Monaco AP, Bertelson CJ, Liechti-Gallati S, Moser H, Kunkel LM (1988) An explanation for the phenotypic differences between patients bearing partial deletions of the DMD locus. *Genomics* 2:90–95.
5. Hoffman EP, Kunkel LM (1989) Dystrophin abnormalities in Duchenne/Becker muscular dystrophy. *Neuron* 2:1019–1029.
6. Eagle M, et al. (2002) Survival in Duchenne muscular dystrophy: Improvements in life expectancy since 1967 and the impact of home nocturnal ventilation. *Neuromuscul Disord* 12:926–929.
7. Chamberlain JR, Chamberlain JS (2017) Progress toward gene therapy for Duchenne muscular dystrophy. *Mol Ther* 25:1125–1131.
8. Ahn AH, Kunkel LM (1993) The structural and functional diversity of dystrophin. *Nat Genet* 3:283–291.
9. Odom GL, Gregorevic P, Chamberlain JS (2007) Viral-mediated gene therapy for the muscular dystrophies: Successes, limitations and recent advances. *Biochim Biophys Acta* 1772:243–262.
10. England SB, et al. (1990) Very mild muscular dystrophy associated with the deletion of 46% of dystrophin. *Nature* 343:180–182.
11. Phelps SF, et al. (1995) Expression of full-length and truncated dystrophin mini-genes in transgenic *mdx* mice. *Hum Mol Genet* 4:1251–1258.
12. Konieczny P, Swiderski K, Chamberlain JS (2013) Gene and cell-mediated therapies for muscular dystrophy. *Muscle Nerve* 47:649–663.
13. Yuasa K, et al. (1998) Effective restoration of dystrophin-associated proteins in vivo by adenovirus-mediated transfer of truncated dystrophin cDNAs. *FEBS Lett* 425:329–336.
14. Harper SQ, et al. (2002) Modular flexibility of dystrophin: Implications for gene therapy of Duchenne muscular dystrophy. *Nat Med* 8:253–261.
15. Braun S, et al. (2000) Immune rejection of human dystrophin following intramuscular injections of naked DNA in mdx mice. *Gene Ther* 7:1447–1457.
16. Wang Z, et al. (2007) Immunity to adeno-associated virus-mediated gene transfer in a random-bred canine model of Duchenne muscular dystrophy. *Hum Gene Ther* 18:18–26.
17. Mendell JR, et al. (2010) Dystrophin immunity in Duchenne's muscular dystrophy. *N Engl J Med* 363:1429–1437.

18. Bulfield G, Siller WG, Wight PA, Moore KJ (1984) X chromosome-linked muscular dystrophy (mdx) in the mouse. *Proc Natl Acad Sci USA* 81:1189–1192.
19. El-Bohy AA, Wong BL (2005) The diagnosis of muscular dystrophy. *Pediatr Ann* 34: 525–530.
20. Brockdorff N, et al. (1987) The mapping of a cDNA from the human X-linked Duchenne muscular dystrophy gene to the mouse X chromosome. *Nature* 328:166–168.
21. Hoffman EP, Morgan JE, Watkins SC, Partridge TA (1990) Somatic reversion/suppression of the mouse *mdx* phenotype in vivo. *J Neurol Sci* 99:9–25.
22. Yucel N, Chang AC, Day JW, Rosenthal N, Blau HM (2018) Humanizing the mdx mouse model of DMD: The long and the short of it. *NPJ Regen Med* 3:4.
23. Sacco A, et al. (2010) Short telomeres and stem cell exhaustion model Duchenne muscular dystrophy in mdx/mTR mice. *Cell* 143:1059–1071.
24. Mourkioti F, et al. (2013) Role of telomere dysfunction in cardiac failure in Duchenne muscular dystrophy. *Nat Cell Biol* 15:895–904.
25. Robinson WH, et al. (2003) Protein microarrays guide tolerizing DNA vaccine treatment of autoimmune encephalomyelitis. *Nat Biotechnol* 21:1033–1039.
26. Solvason N, et al. (2008) Improved efficacy of a tolerizing DNA vaccine for reversal of hyperglycemia through enhancement of gene expression and localization to intracellular sites. *J Immunol* 181:8298–8307.
27. Steinman L (2010) Inverse vaccination, the opposite of Jenner's concept, for therapy of autoimmunity. *J Intern Med* 267:441–451.
28. Garren H, et al. (2001) Combination of gene delivery and DNA vaccination to protect from and reverse Th1 autoimmune disease via deviation to the Th2 pathway. *Immunity* 15:15–22.
29. Gottlieb P, Utz PJ, Robinson W, Steinman L (2013) Clinical optimization of antigen specific modulation of type 1 diabetes with the plasmid DNA platform. *Clin Immunol* 149:297–306.
30. Garren H, et al.; BHT-3009 Study Group (2008) Phase 2 trial of a DNA vaccine encoding myelin basic protein for multiple sclerosis. *Ann Neurol* 63:611–620.
31. Roep BO, et al.; BHT-3021 Investigators (2013) Plasmid-encoded proinsulin preserves C-peptide while specifically reducing proinsulin-specific $CD8^+$ T cells in type 1 diabetes. *Sci Transl Med* 5:191ra82.
32. Bar-Or A, et al. (2007) Induction of antigen-specific tolerance in multiple sclerosis after immunization with DNA encoding myelin basic protein in a randomized, placebo-controlled phase 1/2 trial. *Arch Neurol* 64:1407–1415.
33. Gregorevic P, et al. (2006) rAAV6-microdystrophin preserves muscle function and extends lifespan in severely dystrophic mice. *Nat Med* 12:787–789.
34. Banks GB, Judge LM, Allen JM, Chamberlain JS (2010) The polyproline site in hinge 2 influences the functional capacity of truncated dystrophins. *PLoS Genet* 6:e1000958.
35. Gregorevic P, et al. (2004) Systemic delivery of genes to striated muscles using adeno-associated viral vectors. *Nat Med* 10:828–834.
36. Ho PP, Fontoura P, Ruiz PJ, Steinman L, Garren H (2003) An immunomodulatory GpG oligonucleotide for the treatment of autoimmunity via the innate and adaptive immune systems. *J Immunol* 171:4920–4926.
37. Emery AEH, Muntoni F (2003) *Duchenne Muscular Dystrophy* (Oxford Univ Press, Oxford), 3rd Ed.
38. Finsterer J, Stöllberger C (2003) The heart in human dystrophinopathies. *Cardiology* 99:1–19.
39. de Kermadec JM, Bécane HM, Chénard A, Tertrain F, Weiss Y (1994) Prevalence of left ventricular systolic dysfunction in Duchenne muscular dystrophy: An echocardiographic study. *Am Heart J* 127:618–623.
40. Thomas TO, Morgan TM, Burnette WB, Markham LW (2012) Correlation of heart rate and cardiac dysfunction in Duchenne muscular dystrophy. *Pediatr Cardiol* 33: 1175–1179.
41. Zatz M, Shapiro LJ, Campion DS, Oda E, Kaback MM (1978) Serum pyruvate-kinase (PK) and creatine-phosphokinase (CPK) in progressive muscular dystrophies. *J Neurol Sci* 36:349–362.
42. Zatz M, et al. (1991) Serum creatine-kinase (CK) and pyruvate-kinase (PK) activities in Duchenne (DMD) as compared with Becker (BMD) muscular dystrophy. *J Neurol Sci* 102:190–196.
43. Vandamme C, Adjali O, Mingozzi F (2017) Unraveling the complex story of immune responses to AAV vectors trial after trial. *Hum Gene Ther* 28:1061–1074.
44. Bies RD, et al. (1992) Human and murine dystrophin mRNA transcripts are differentially expressed during skeletal muscle, heart, and brain development. *Nucleic Acids Res* 20:1725–1731.
45. Tusher VG, Tibshirani R, Chu G (2001) Significance analysis of microarrays applied to the ionizing radiation response. *Proc Natl Acad Sci USA* 98:5116–5121.
46. Eisen MB, Spellman PT, Brown PO, Botstein D (1998) Cluster analysis and display of genome-wide expression patterns. *Proc Natl Acad Sci USA* 95:14863–14868.
47. Nakamura A (2017) Moving towards successful exon-skipping therapy for Duchenne muscular dystrophy. *J Hum Genet* 62:871–876.
48. Ousterout DG, et al. (2015) Multiplex CRISPR/Cas9-based genome editing for correction of dystrophin mutations that cause Duchenne muscular dystrophy. *Nat Commun* 6:6244.
49. Long C, et al. (2016) Postnatal genome editing partially restores dystrophin expression in a mouse model of muscular dystrophy. *Science* 351:400–403.
50. Nelson CE, et al. (2016) In vivo genome editing improves muscle function in a mouse model of Duchenne muscular dystrophy. *Science* 351:403–407.
51. Tabebordbar M, et al. (2016) In vivo gene editing in dystrophic mouse muscle and muscle stem cells. *Science* 351:407–411.
52. Amoasii L, et al. (2017) Single-cut genome editing restores dystrophin expression in a new mouse model of muscular dystrophy. *Sci Transl Med* 9:eaan8081.
53. Bengtsson NE, et al. (2017) Muscle-specific CRISPR/Cas9 dystrophin gene editing ameliorates pathophysiology in a mouse model for Duchenne muscular dystrophy. *Nat Commun* 8:14454.
54. Kayali R, Bury F, Ballard M, Bertoni C (2010) Site-directed gene repair of the dystrophin gene mediated by PNA-ssODNs. *Hum Mol Genet* 19:3266–3281.
55. Nik-Ahd F, Bertoni C (2014) Ex vivo gene editing of the dystrophin gene in muscle stem cells mediated by peptide nucleic acid single stranded oligodeoxynucleotides induces stable expression of dystrophin in a mouse model for Duchenne muscular dystrophy. *Stem Cells* 32:1817–1830.
56. Urish K, Kanda Y, Huard J (2005) Initial failure in myoblast transplantation therapy has led the way toward the isolation of muscle stem cells: Potential for tissue regeneration. *Curr Top Dev Biol* 68:263–280.
57. Karpati G, et al. (1989) Dystrophin is expressed in mdx skeletal muscle fibers after normal myoblast implantation. *Am J Pathol* 135:27–32.
58. Partridge TA, Morgan JE, Coulton GR, Hoffman EP, Kunkel LM (1989) Conversion of mdx myofibres from dystrophin-negative to -positive by injection of normal myoblasts. *Nature* 337:176–179.
59. Gussoni E, et al. (1992) Normal dystrophin transcripts detected in Duchenne muscular dystrophy patients after myoblast transplantation. *Nature* 356:435–438.
60. Gussoni E, Blau HM, Kunkel LM (1997) The fate of individual myoblasts after transplantation into muscles of DMD patients. *Nat Med* 3:970–977.
61. Karpati G, et al. (1993) Myoblast transfer in Duchenne muscular dystrophy. *Ann Neurol* 34:8–17.
62. Mendell JR, et al. (1995) Myoblast transfer in the treatment of Duchenne's muscular dystrophy. *N Engl J Med* 333:832–838.
63. Miller RG, et al. (1997) Myoblast implantation in Duchenne muscular dystrophy: The San Francisco study. *Muscle Nerve* 20:469–478.
64. Hartigan-O'Connor D, Kirk CJ, Crawford R, Mulé JJ, Chamberlain JS (2001) Immune evasion by muscle-specific gene expression in dystrophic muscle. *Mol Ther* 4:525–533.
65. Lai Y, et al. (2005) Efficient in vivo gene expression by trans-splicing adeno-associated viral vectors. *Nat Biotechnol* 23:1435–1439.
66. Klein CJ, et al. (1992) Somatic reversion/suppression in Duchenne muscular dystrophy (DMD): Evidence supporting a frame-restoring mechanism in rare dystrophin-positive fibers. *Am J Hum Genet* 50:950–959.
67. Manno CS, et al. (2006) Successful transduction of liver in hemophilia by AAV-factor IX and limitations imposed by the host immune response. *Nat Med* 12:342–347, and erratum (2006) 12:592.
68. Snyder RO, et al. (1999) Correction of hemophilia B in canine and murine models using recombinant adeno-associated viral vectors. *Nat Med* 5:64–70.
69. Wang L, Nichols TC, Read MS, Bellinger DA, Verma IM (2000) Sustained expression of therapeutic level of factor IX in hemophilia B dogs by AAV-mediated gene therapy in liver. *Mol Ther* 1:154–158.
70. Wang Z, et al. (2007) Sustained AAV-mediated dystrophin expression in a canine model of Duchenne muscular dystrophy with a brief course of immunosuppression. *Mol Ther* 15:1160–1166.
71. Gregorevic P, Blankinship MJ, Allen JM, Chamberlain JS (2008) Systemic microdystrophin gene delivery improves skeletal muscle structure and function in old dystrophic *mdx* mice. *Mol Ther* 16:657–664.
72. Sabatino DE, et al. (2005) Identification of mouse AAV capsid-specific CD8+ T cell epitopes. *Mol Ther* 12:1023–1033.
73. Chirmule N, et al. (2000) Humoral immunity to adeno-associated virus type 2 vectors following administration to murine and nonhuman primate muscle. *J Virol* 74: 2420–2425.
74. Yuasa K, et al. (2002) Adeno-associated virus vector-mediated gene transfer into dystrophin-deficient skeletal muscles evokes enhanced immune response against the transgene product. *Gene Ther* 9:1576–1588.
75. Ferrer A, Foster H, Wells KE, Dickson G, Wells DJ (2004) Long-term expression of full-length human dystrophin in transgenic mdx mice expressing internally deleted human dystrophins. *Gene Ther* 11:884–893.
76. Ramos J, Chamberlain JS (2015) Gene therapy for Duchenne muscular dystrophy. *Expert Opin Orphan Drugs* 3:1255–1266.
77. Song X, et al. (2009) Construction and characterization of a novel DNA vaccine that is potent antigen-specific tolerizing therapy for experimental arthritis by increasing CD4+CD25+Treg cells and inducing Th1 to Th2 shift in both cells and cytokines. *Vaccine* 27:690–700.
78. Chicoine LG, et al. (2014) Plasmapheresis eliminates the negative impact of AAV antibodies on microdystrophin gene expression following vascular delivery. *Mol Ther* 22:338–347.
79. Filareto A, et al. (2013) An ex vivo gene therapy approach to treat muscular dystrophy using inducible pluripotent stem cells. *Nat Commun* 4:1549.